

Calculation of the amplitude matrix for a nonspherical particle in a fixed orientation

Michael I. Mishchenko

General equations are derived for computing the amplitude matrix for a nonspherical particle in an arbitrary orientation and for arbitrary illumination and scattering directions with respect to the laboratory reference frame, provided that the scattering problem can be solved with respect to the particle reference frame. These equations are used along with the *T*-matrix method to provide benchmark results for homogeneous, dielectric, rotationally symmetric particles. The computer code is publicly available on the World-Wide Web at <http://www.giss.nasa.gov/~crmim>.

OCIS codes: 010.1310, 290.0290, 290.1310, 290.4210, 290.5850.

1. Introduction

Many practical applications require the knowledge of electromagnetic scattering characteristics of perfectly or partially oriented nonspherical particles for arbitrary directions of the incident and scattered beams. Most of the available analytical and numerical techniques assume that (or become especially efficient when) the scattering problem is solved in the particle reference frame with coordinate axes directed along the axes of particle symmetry.¹ However, it is often necessary to use a fixed laboratory coordinate system to specify both the directions of the incident and scattered beams and the particle orientation, for example, for solving the vector radiative transfer equation for preferentially oriented nonspherical particles such as hydrometeors and interstellar dust grains.²⁻⁴ In this case one has first to determine the illumination and scattering directions with respect to the particle reference frame for a given orientation of the particle relative to the laboratory reference frame, then solve the scattering problem in the particle reference frame, and finally perform the backward transition to the laboratory reference frame. In this paper we shall derive general formulas that describe this procedure and use them along with the *T*-matrix method to provide benchmark results that could be useful for testing purposes. Unlike in Refs. 5 and 6, we shall permit

arbitrary directions of the incident and scattered beams with respect to the laboratory reference frame rather than assume that the illumination direction is along the positive *z* axis and that the scattering direction is confined to the *xz* plane.

2. Reference Frames and Particle Orientation

To describe the scattering of a plane electromagnetic wave by a nonspherical particle in an arbitrary orientation, one must first specify the directions of the incident and scattered waves and the orientation of the particle with respect to a laboratory reference frame. Let this reference frame be a right-handed Cartesian coordinate system *L* with orientation fixed in space, having its origin inside the particle. The direction of propagation of a transverse electromagnetic wave is specified by a unit vector \hat{n} or, equivalently, by a couple (ϑ_L, φ_L) , where $\vartheta_L \in [0, \pi]$ is the polar (zenith) angle measured from the positive *z* axis and $\varphi_L \in [0, 2\pi]$ is the azimuth angle measured from the positive *x* axis in the clockwise sense, when one is looking in the direction of the positive *z* axis (Fig. 1). The ϑ and φ components of the electric field are denoted $\mathbf{E}_{\vartheta L}$ and $\mathbf{E}_{\varphi L}$, respectively. The component $\mathbf{E}_{\vartheta L} = E_{\vartheta L} \hat{\vartheta}_L$ lies in the meridional plane (plane through the beam and the *z* axis), whereas the component $\mathbf{E}_{\varphi L} = E_{\varphi L} \hat{\varphi}_L$ is perpendicular to this plane, where $\hat{\vartheta}_L$ and $\hat{\varphi}_L$ are the corresponding unit vectors such that

$$\hat{n} = \hat{\vartheta}_L \times \hat{\varphi}_L. \quad (1)$$

Note that $\mathbf{E}_{\vartheta L}$ and $\mathbf{E}_{\varphi L}$ are also often denoted \mathbf{E}_v and \mathbf{E}_h and called the vertical and horizontal electric field vector components, respectively.²

The author is with the NASA Goddard Institute for Space Studies, 2880 Broadway, New York, New York 10025. His e-mail address is crmim@giss.nasa.gov.

Received 10 August 1999; revised manuscript received 8 November 1999.

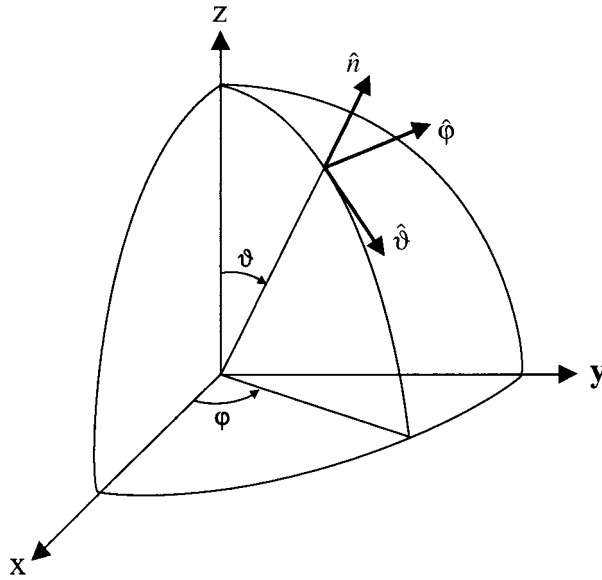


Fig. 1. Spherical coordinate system used to specify the direction and the polarization state of a transverse electromagnetic wave.

To specify the orientation of the particle with respect to the laboratory reference frame, we introduce a right-handed coordinate system P fixed to the particle and having the same origin as L . This coordinate system will be called the particle reference frame. The orientation of the particle with respect to the laboratory frame, L , is specified by three Euler angles of rotation, α , β , and γ , that transform the coordinate system $L\{x, y, z\}$ into the coordinate system $P\{x', y', z'\}$, as shown in Fig. 2 (Chap. 1 of Ref. 1 and Ref. 7). The three consecutive Euler rotations are performed as follows:

- Rotation about the z axis through an angle $\alpha \in [0, 2\pi)$, reorienting the y axis such that it coincides

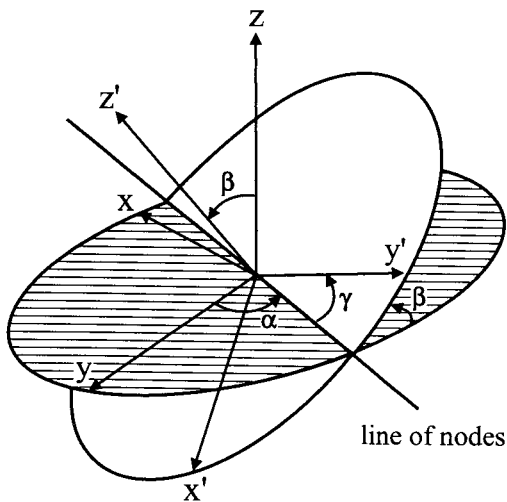


Fig. 2. Transformation of the laboratory reference system xyz into the particle reference frame $x'y'z'$.

with the line of nodes (line formed by the intersection of the xy and $x'y'$ planes),

- Rotation about the new y axis through an angle $\beta \in [0, \pi]$,
- Rotation about the z' axis through an angle $\gamma \in [0, 2\pi)$.

An angle of rotation is positive if the rotation is in the clockwise direction when one is looking in the positive direction of the rotation axis.

3. Amplitude Matrix in the Laboratory Reference Frame

Throughout this paper we assume and suppress the time-harmonic factor $\exp(-i\omega t)$. Consider a monochromatic plane electromagnetic wave with electric field vector

$$\mathbf{E}^{\text{inc}}(\mathbf{R}) = (E_{\partial L}^{\text{inc}} \hat{\delta}_L^{\text{inc}} + E_{\phi L}^{\text{inc}} \hat{\phi}_L^{\text{inc}}) \exp(ik\hat{n}^{\text{inc}} \cdot \mathbf{R}) \quad (2)$$

incident upon a nonspherical particle in a direction \hat{n}^{inc} ; here $i = \sqrt{-1}$, $k = 2\pi/\lambda$ is the free-space wave number, λ is the free-space wavelength, \mathbf{R} is the position vector connecting the origin of the laboratory coordinate system and the observation point, and the subscript L labels vector components computed in the laboratory reference frame. Because of the linearity of Maxwell's equations and boundary conditions, it is always possible to express the scattered electric field linearly in the incident electric field. In the far-field region ($kR \gg 1$, $R = |\mathbf{R}|$), the scattered wave becomes spherical and is given by²

$$\mathbf{E}^{\text{sca}}(\mathbf{R}) = E_{\partial L}^{\text{sca}}(R, \hat{n}^{\text{sca}}) \hat{\delta}_L^{\text{sca}} + E_{\phi L}^{\text{sca}}(R, \hat{n}^{\text{sca}}) \hat{\phi}_L^{\text{sca}},$$

$$\hat{n}^{\text{sca}} = \frac{\mathbf{R}}{R} = \hat{\delta}_L^{\text{sca}} \times \hat{\phi}_L^{\text{sca}}, \quad (3)$$

$$\hat{n}^{\text{sca}} \cdot \mathbf{E}^{\text{sca}}(\mathbf{R}) = 0, \quad (4)$$

$$\begin{bmatrix} E_{\partial L}^{\text{sca}} \\ E_{\phi L}^{\text{sca}} \end{bmatrix} = \frac{\exp(ikR)}{R} \mathbf{S}^L(\hat{n}^{\text{sca}}, \hat{n}^{\text{inc}}, \alpha, \beta, \gamma) \begin{bmatrix} E_{\partial L}^{\text{inc}} \\ E_{\phi L}^{\text{inc}} \end{bmatrix}, \quad (5)$$

where \mathbf{S}^L is a 2×2 amplitude matrix that transforms the electric field vector components of the incident wave into the electric field vector components of the scattered wave in the laboratory reference frame. The amplitude matrix depends on the directions of incidence and scattering as well as on the size, morphology, and composition of the scattering particle and on its orientation with respect to the laboratory reference frame as specified by the Euler angles of rotation α , β , and γ .

4. Reference Frame Transformations

Assume that one can use one of the available analytical or numerical techniques (e.g., in Chap. 2 of Ref. 1) to find the amplitude matrix with respect to the particle reference frame. This matrix will be denoted \mathbf{S}^P and relates the incident and scattered field vector

components computed in the particle reference frame:

$$\begin{bmatrix} E_{\vartheta P}^{\text{sca}} \\ E_{\varphi P}^{\text{sca}} \end{bmatrix} = \frac{\exp(ikR)}{R} \mathbf{S}^P(\hat{n}^{\text{sca}}, \hat{n}^{\text{inc}}) \begin{bmatrix} E_{\vartheta P}^{\text{inc}} \\ E_{\varphi P}^{\text{inc}} \end{bmatrix}. \quad (6)$$

The amplitude matrix with respect to the laboratory reference frame can be expressed in terms of the matrix \mathbf{S}^P as follows: Denote by $\hat{\rho}$ a 2×2 matrix that transforms the electric field vector components of a transverse electromagnetic wave computed in the laboratory reference frame into those computed in the particle reference frame:

$$\begin{bmatrix} E_{\vartheta P}(\vartheta_P, \varphi_P) \\ E_{\varphi P}(\vartheta_P, \varphi_P) \end{bmatrix} = \hat{\rho}(\hat{n}; \alpha, \beta, \gamma) \begin{bmatrix} E_{\vartheta L}(\vartheta_L, \varphi_L) \\ E_{\varphi L}(\vartheta_L, \varphi_L) \end{bmatrix}, \quad (7)$$

where \hat{n} is a unit vector in the direction of light propagation, whereas (ϑ_L, φ_L) and (ϑ_P, φ_P) specify this direction with respect to the laboratory and particle reference frames, respectively. The $\hat{\rho}$ matrix de-

$$\hat{\beta}(\alpha, \beta, \gamma) = \begin{bmatrix} \cos \alpha \cos \beta \cos \gamma - \sin \alpha \sin \gamma & \sin \alpha \cos \beta \cos \gamma + \cos \alpha \sin \gamma & -\sin \beta \cos \gamma \\ -\cos \alpha \cos \beta \sin \gamma - \sin \alpha \cos \gamma & -\sin \alpha \cos \beta \sin \gamma + \cos \alpha \cos \gamma & \sin \beta \sin \gamma \\ \cos \alpha \sin \beta & \sin \alpha \sin \beta & \cos \beta \end{bmatrix}. \quad (17)$$

pends on \hat{n} as well as on the orientation of the particle relative to the laboratory reference frame, as given by Euler angles α , β , and γ . We can then easily derive

$$\mathbf{S}^L(\vartheta_L^{\text{sca}}, \varphi_L^{\text{sca}}; \vartheta_L^{\text{inc}}, \varphi_L^{\text{inc}}; \alpha, \beta, \gamma) = \hat{\rho}^{-1}(\hat{n}^{\text{sca}}; \alpha, \beta, \gamma) \times \mathbf{S}^P(\vartheta_P^{\text{sca}}, \varphi_P^{\text{sca}}; \vartheta_P^{\text{inc}}, \varphi_P^{\text{inc}}) \hat{\rho}(\hat{n}^{\text{inc}}; \alpha, \beta, \gamma). \quad (8)$$

Angles ϑ_P and φ_P are expressed in terms of angles ϑ_L and φ_L as

$$\cos \vartheta_P = \cos \vartheta_L \cos \beta + \sin \vartheta_L \sin \beta \cos(\varphi_L - \alpha), \quad (9)$$

$$\begin{aligned} \cos \varphi_P &= \frac{1}{\sin \vartheta_P} [\cos \beta \cos \gamma \sin \vartheta_L \cos(\varphi_L - \alpha) \\ &+ \sin \gamma \sin \vartheta_L \sin(\varphi_L - \alpha) \\ &- \sin \beta \cos \gamma \cos \vartheta_L], \end{aligned} \quad (10)$$

$$\begin{aligned} \sin \varphi_P &= \frac{1}{\sin \vartheta_P} [-\cos \beta \sin \gamma \sin \vartheta_L \cos(\varphi_L - \alpha) \\ &+ \cos \gamma \sin \vartheta_L \sin(\varphi_L - \alpha) \\ &+ \sin \beta \sin \gamma \cos \vartheta_L]. \end{aligned} \quad (11)$$

To determine the $\hat{\rho}$ matrix, we proceed as follows: Denote by $\hat{\alpha}$ a 3×2 matrix that transforms the ϑ and φ components of the electric field vector into its x , y , and z components:

$$\begin{bmatrix} E_x \\ E_y \\ E_z \end{bmatrix} = \hat{\alpha}(\vartheta, \varphi) \begin{bmatrix} E_{\vartheta} \\ E_{\varphi} \end{bmatrix}, \quad (12)$$

and by $\hat{\beta}$ a 3×3 matrix that expresses the x , y , and z components of a vector in the particle coordinate system in the x , y , and z components of the same vector in the laboratory coordinate system:

$$\begin{bmatrix} E_{xP} \\ E_{yP} \\ E_{zP} \end{bmatrix} = \hat{\beta}(\alpha, \beta, \gamma) \begin{bmatrix} E_{xL} \\ E_{yL} \\ E_{zL} \end{bmatrix}. \quad (13)$$

We then finally have

$$\hat{\rho}(\hat{n}; \alpha, \beta, \gamma) = \hat{\alpha}^{-1}(\vartheta_P, \varphi_P) \hat{\beta}(\alpha, \beta, \gamma) \hat{\alpha}(\vartheta_L, \varphi_L). \quad (14)$$

The matrices that enter the right-hand side of Eq. (14) are as follows⁷:

$$\hat{\alpha}(\vartheta, \varphi) = \begin{bmatrix} \cos \vartheta \cos \varphi & -\sin \varphi \\ \cos \vartheta \sin \varphi & \cos \varphi \\ -\sin \vartheta & 0 \end{bmatrix}, \quad (15)$$

$$\hat{\alpha}^{-1}(\vartheta, \varphi) = \begin{bmatrix} \cos \vartheta \cos \varphi & \cos \vartheta \sin \varphi & -\sin \vartheta \\ -\sin \varphi & \cos \varphi & 0 \end{bmatrix}, \quad (16)$$

One can easily verify that, if the particle reference frame coincides with the laboratory reference frame, then

$$\hat{\rho}(\hat{n}; \alpha = 0, \beta = 0, \gamma = 0) \equiv \begin{bmatrix} 1 & 0 \\ 0 & 1 \end{bmatrix}, \quad (18)$$

$$\mathbf{S}^L(\vartheta_L^{\text{sca}}, \varphi_L^{\text{sca}}; \vartheta_L^{\text{inc}}, \varphi_L^{\text{inc}}; 0, 0, 0) = \mathbf{S}^P(\vartheta_P^{\text{sca}}, \varphi_P^{\text{sca}}; \vartheta_P^{\text{inc}}, \varphi_P^{\text{inc}}). \quad (19)$$

For rotationally symmetric particles it is advantageous to choose the particle coordinate system such that its z axis is directed along the axis of particle symmetry. In this case the orientation of the particle with respect to the laboratory coordinate system is independent of Euler angle γ , so we can set $\gamma = 0$ and get, instead of Eqs. (10), (11), and (17),

$$\begin{aligned} \cos \varphi_P &= \frac{1}{\sin \vartheta_P} [\cos \beta \sin \vartheta_L \cos(\varphi_L - \alpha) \\ &- \sin \beta \cos \vartheta_L], \end{aligned} \quad (20)$$

$$\sin \varphi_P = \frac{\sin \vartheta_L \sin(\varphi_L - \alpha)}{\sin \vartheta_P}, \quad (21)$$

$$\hat{\beta}(\alpha, \beta, \gamma = 0) = \begin{bmatrix} \cos \alpha \cos \beta & \sin \alpha \cos \beta & -\sin \beta \\ -\sin \alpha & \cos \alpha & 0 \\ \cos \alpha \sin \beta & \sin \alpha \sin \beta & \cos \beta \end{bmatrix}. \quad (22)$$

5. Amplitude Matrix in the Particle Reference Frame

It is rather convenient to compute the amplitude matrix with respect to the particle reference frame by using the T -matrix method^{8,9} because, for rotationally symmetric particles, the T matrix is diagonal with respect to the azimuthal indices m and m' :

$$T_{mnm'n'}^{kl}(P) = \delta_{mm'} T_{mnmn'}^{kl}(P), \quad k, l = 1, 2, \quad (23)$$

where $\delta_{mm'}$ is the Kronecker delta. We therefore have

$$\begin{aligned} S_{11}^P(\hat{n}^{\text{sca}}, \hat{n}^{\text{inc}}) &= \frac{1}{k} \sum_{n=1}^{\infty} \sum_{n'=1}^{\infty} \sum_{m=-\min(n,n')}^{\min(n,n')} \\ &\times \alpha_{mnn'} [T_{mnmn'}^{11}(P) \pi_{mn}(\vartheta^{\text{sca}}) \pi_{mn'}(\vartheta^{\text{inc}}) \\ &+ T_{mnmn'}^{21}(P) \tau_{mn}(\vartheta^{\text{sca}}) \pi_{mn'}(\vartheta^{\text{inc}}) \\ &+ T_{mnmn'}^{12}(P) \pi_{mn}(\vartheta^{\text{sca}}) \tau_{mn'}(\vartheta^{\text{inc}}) \\ &+ T_{mnmn'}^{22}(P) \tau_{mn}(\vartheta^{\text{sca}}) \tau_{mn'}(\vartheta^{\text{inc}})], \quad (24) \end{aligned}$$

$$\begin{aligned} S_{12}^P(\hat{n}^{\text{sca}}, \hat{n}^{\text{inc}}) &= -\frac{i}{k} \sum_{n=1}^{\infty} \sum_{n'=1}^{\infty} \sum_{m=-\min(n,n')}^{\min(n,n')} \\ &\times \alpha_{mnn'} [T_{mnmn'}^{11}(P) \pi_{mn}(\vartheta^{\text{sca}}) \tau_{mn'}(\vartheta^{\text{inc}}) \\ &+ T_{mnmn'}^{21}(P) \tau_{mn}(\vartheta^{\text{sca}}) \tau_{mn'}(\vartheta^{\text{inc}}) \\ &+ T_{mnmn'}^{12}(P) \pi_{mn}(\vartheta^{\text{sca}}) \pi_{mn'}(\vartheta^{\text{inc}}) \\ &+ T_{mnmn'}^{22}(P) \tau_{mn}(\vartheta^{\text{sca}}) \pi_{mn'}(\vartheta^{\text{inc}})], \quad (25) \end{aligned}$$

$$\begin{aligned} S_{21}^P(\hat{n}^{\text{sca}}, \hat{n}^{\text{inc}}) &= \frac{i}{k} \sum_{n=1}^{\infty} \sum_{n'=1}^{\infty} \sum_{m=-\min(n,n')}^{\min(n,n')} \\ &\times \alpha_{mnn'} [T_{mnmn'}^{11}(P) \tau_{mn}(\vartheta^{\text{sca}}) \pi_{mn'}(\vartheta^{\text{inc}}) \\ &+ T_{mnmn'}^{21}(P) \pi_{mn}(\vartheta^{\text{sca}}) \pi_{mn'}(\vartheta^{\text{inc}}) \\ &+ T_{mnmn'}^{12}(P) \tau_{mn}(\vartheta^{\text{sca}}) \tau_{mn'}(\vartheta^{\text{inc}}) \\ &+ T_{mnmn'}^{22}(P) \pi_{mn}(\vartheta^{\text{sca}}) \tau_{mn'}(\vartheta^{\text{inc}})], \quad (26) \end{aligned}$$

$$\begin{aligned} S_{22}^P(\hat{n}^{\text{sca}}, \hat{n}^{\text{inc}}) &= \frac{1}{k} \sum_{n=1}^{\infty} \sum_{n'=1}^{\infty} \sum_{m=-\min(n,n')}^{\min(n,n')} \\ &\times \alpha_{mnn'} [T_{mnmn'}^{11}(P) \tau_{mn}(\vartheta^{\text{sca}}) \tau_{mn'}(\vartheta^{\text{inc}}) \\ &+ T_{mnmn'}^{21}(P) \pi_{mn}(\vartheta^{\text{sca}}) \tau_{mn'}(\vartheta^{\text{inc}}) \\ &+ T_{mnmn'}^{12}(P) \tau_{mn}(\vartheta^{\text{sca}}) \pi_{mn'}(\vartheta^{\text{inc}}) \\ &+ T_{mnmn'}^{22}(P) \pi_{mn}(\vartheta^{\text{sca}}) \pi_{mn'}(\vartheta^{\text{inc}})], \quad (27) \end{aligned}$$

where

$$\begin{aligned} \alpha_{mnn'} &= i^{n'-n-1} \left[\frac{(2n+1)(2n'+1)}{n(n+1)n'(n'+1)} \right]^{1/2} \\ &\times \exp[im(\varphi^{\text{sca}} - \varphi^{\text{inc}})], \quad (28) \end{aligned}$$

$$\pi_{mn}(\vartheta) = \frac{m d_{0m}^n(\vartheta)}{\sin \vartheta}, \quad \tau_{mn}(\vartheta) = \frac{d d_{0m}^n(\vartheta)}{d\vartheta}, \quad (29)$$

and $d_{m'm}^n(\vartheta)$ are Wigner d functions.⁷

Note that the amplitude matrix is often expressed in terms of associated Legendre functions:

$$P_n^m(\cos \vartheta) = (-1)^m \left[\frac{(n+m)!}{(n-m)!} \right]^{1/2} d_{0m}^n(\vartheta), \quad (30)$$

rather than in terms of Wigner d functions (see, e.g., Ref. 2), although it is well known that the numerical computation of associated Legendre functions with large m and n is unstable and leads to overflows.¹⁰ However, the computation of the Wigner d functions by means of the upward recurrence relation⁷

$$\begin{aligned} [(n+1)^2 - m^2]^{1/2} d_{0m}^{n+1}(\vartheta) &= (2n+1) \cos \vartheta d_{0m}^n(\vartheta) \\ &- \sqrt{n^2 - m^2} d_{0m}^{n-1}(\vartheta) \quad (31) \end{aligned}$$

and the initial conditions

$$d_{0m}^{m-1}(\vartheta) = 0, \quad (32)$$

$$d_{0m}^m(\vartheta) = A_m (1 - \cos^2 \vartheta)^{m/2}, \quad (33)$$

$$A_0 = 1, \quad A_{m+1} = A_m \left[\frac{2m+1}{2(m+1)} \right]^{1/2} \quad (34)$$

is numerically stable and efficient. The function $\tau_{mn}(\vartheta)$ can then be found from

$$\begin{aligned} \tau_{mn}(\vartheta) &= \frac{1}{(2n+1) \sin \vartheta} \{ -(n+1) \sqrt{n^2 - m^2} d_{0m}^{n-1}(\vartheta) \\ &+ [(n+1)^2 - m^2]^{1/2} d_{0m}^{n+1}(\vartheta) \}. \quad (35) \end{aligned}$$

Many practical aspects of T -matrix computations are discussed in Ref. 11.

6. Numerical Scheme

Assuming that the scattering particle is rotationally symmetric and that the axis of symmetry is directed along the z axis of the particle reference frame, we can summarize the numerical scheme for computing the amplitude matrix for given $\vartheta_L^{\text{inc}}, \varphi_L^{\text{inc}}, \vartheta_L^{\text{sca}}, \varphi_L^{\text{sca}}, \alpha, \beta$, and $\gamma = 0$ as follows:

- Calculation of $\vartheta_P^{\text{inc}}, \varphi_P^{\text{inc}}, \vartheta_P^{\text{sca}}$, and φ_P^{sca} by Eqs. (9), (20), and (21),
- Calculation of the matrix $\hat{\beta}(\alpha, \beta, \gamma = 0)$ by Eq. (22),
- Calculation of the matrices $\hat{\alpha}(\vartheta_L^{\text{inc}}, \varphi_L^{\text{inc}}), \hat{\alpha}(\vartheta_L^{\text{sca}}, \varphi_L^{\text{sca}}), \hat{\alpha}^{-1}(\vartheta_P^{\text{inc}}, \varphi_P^{\text{inc}})$, and $\hat{\alpha}^{-1}(\vartheta_P^{\text{sca}}, \varphi_P^{\text{sca}})$ by Eqs. (15) and (16),
- Calculation of the matrices $\hat{\rho}(\hat{n}^{\text{inc}}; \alpha, \beta, \gamma)$ and $\hat{\rho}^{-1}(\hat{n}^{\text{sca}}; \alpha, \beta, \gamma)$ by Eq. (14),
- Calculation of the matrix $\mathbf{S}^P(\vartheta_P^{\text{sca}}, \varphi_P^{\text{sca}}, \vartheta_P^{\text{inc}}, \varphi_P^{\text{inc}})$ by Eqs. (24)–(27),
- Calculation of the matrix $\mathbf{S}^L(\vartheta_L^{\text{sca}}, \varphi_L^{\text{sca}}, \vartheta_L^{\text{inc}}, \varphi_L^{\text{inc}}; \alpha, \beta, 0)$ by Eq. (8).

7. Benchmark Results

In this section I present the results of T -matrix computations for the following four rotationally symmetric particles:

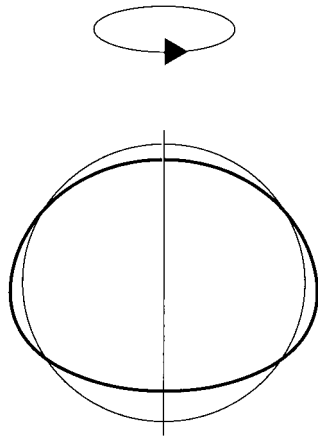


Fig. 3. Thick curve, the shape of the generalized Chebyshev particle used in the computation of expression (40); thin curve, the equal-volume sphere.

- prolate spheroid with an aspect ratio of 2,
- circular cylinder with a length-to-diameter ratio of 2,
- Chebyshev particle with degree 4 and deformation parameter 0.1,^{6,11}
- generalized Chebyshev particle with shape given by

$$r(\vartheta, \varphi) = r_0 \left[1 + \sum_{n=0}^N c_n \cos(n\vartheta) \right], \quad (36)$$

with $N = 10$, $c_0 = -0.0481$, $c_1 = 0.0359$, $c_2 = -0.1263$, $c_3 = 0.0244$, $c_4 = 0.0091$, $c_5 = -0.0099$, $c_6 = 0.0015$, $c_7 = 0.0025$, $c_8 = -0.0016$, $c_9 = -0.0002$, and $c_{10} = 0.0010$ (Fig. 3).

Note that generalized Chebyshev particles are often used to describe the shape of distorted raindrops.^{4,12,13} The surface-equivalent-sphere radius for the first three particles and equal-volume-sphere radius for the fourth particle is $10 \mu\text{m}$. All particles have the same refractive index, $1.5 + 0.02i$, and the same orientation with respect to the laboratory reference frame, given by $\alpha = 145^\circ$ and $\beta = 52^\circ$. The directions of the incident and scattered beams relative to the laboratory reference frame are given by the angles $\vartheta_L^{\text{inc}} = 56^\circ$, $\varphi_L^{\text{inc}} = 114^\circ$, $\vartheta_L^{\text{sca}} = 65^\circ$, and $\varphi_L^{\text{sca}} = 128^\circ$. The wavelength of the incident light is $6.283185 \mu\text{m}$. The respective amplitude matrices (with elements given in micrometers) are as follows:

$$\begin{bmatrix} -5.0941 + 24.402i & -1.9425 + 1.9971i \\ -1.1521 - 3.0978i & -6.9323 + 24.748i \end{bmatrix}, \quad (37)$$

$$\begin{bmatrix} -1.727 + 19.706i & -0.562 + 0.247i \\ -2.013 - 2.398i & -3.088 + 20.401i \end{bmatrix}, \quad (38)$$

$$\begin{bmatrix} 4.5123 + 18.092i & -1.6350 + 3.5274i \\ -3.0970 - 0.9215i & 3.2658 + 18.617i \end{bmatrix}, \quad (39)$$

$$\begin{bmatrix} 11.307 + 9.6184i & -2.6519 + 2.3589i \\ -4.9044 - 0.6241i & 9.9947 + 11.295i \end{bmatrix}. \quad (40)$$

These numbers are expected to be accurate to within ± 2 in the last digits given.

To provide an additional test of the accuracy of the computer code for particles in a fixed orientation, I used it to calculate the elements of the scattering matrix for a uniform orientation distribution by numerically evaluating the respective angular integrals. These results were then compared with those rendered by the code based on an analytical averaging method for randomly oriented particles.^{11,14} Inasmuch as the latter technique completely avoids the evaluation of the amplitude matrix for specific particle orientations and illumination and scattering directions, it provides an excellent independent check. The perfect agreement found (five and more significant digits) suggests that both codes provide high numerical accuracy and can be used in practical applications as well as sources of benchmark results for testing various numerical techniques.

8. Summary

In this paper we have derived general formulas that can be used to compute the amplitude matrix for an arbitrary orientation of a nonspherical particle and arbitrary directions of illumination and scattering with respect to the laboratory reference frame, provided that the electromagnetic scattering problem can be solved in the particle reference frame. These formulas become especially simple for rotationally symmetric particles and have been used along with the T -matrix method to compute benchmark results for four dielectric, rotationally symmetric particles in a fixed orientation. The FORTRAN computer code is publicly available on the World-Wide Web at <http://www.giss.nasa.gov/~crmim> in both the double-precision and the extended-precision versions. The former version is significantly faster, whereas the latter version can be applied to significantly larger particles.^{9,11}

An important advantage of the T -matrix method is that the T matrix for a given nonspherical particle needs to be computed only once and can then be used for any directions of incidence and scattering and for any orientations of the particle with respect to the laboratory reference frame. This simplicity of the method allows one to easily calculate orientationally averaged extinction and phase matrices entering the general vector radiative transfer equation (see, e.g., Chap. 1 of Ref. 1 and Refs. 2–4). Of course, additional averaging over particle shapes and sizes will require a separate computation of the T matrix for each particle species.

I thank Timo Nousiainen and two anonymous referees for their comments on an earlier version of this paper and Lilly Del Valle and Nadia Zakharova for help with the graphics. This research was sponsored by the NASA Radiation Science Program managed by Robert Curran.

References

1. M. I. Mishchenko, J. W. Hovenier, and L. D. Travis, eds., *Light Scattering by Nonspherical Particles: Theory, Measurements, and Applications* (Academic, San Diego, Calif., 1999).
2. L. Tsang, J. A. Kong, and R. T. Shin, *Theory of Microwave Remote Sensing* (Wiley, New York, 1985).
3. M. I. Mishchenko, "Multiple scattering of polarized light in anisotropic plane-parallel media," *Transp. Theory Stat. Phys.* **19**, 293–316 (1990).
4. J. L. Haferman, "Microwave scattering by precipitation," in *Light Scattering by Nonspherical Particles: Theory, Measurements, and Applications*, M. I. Mishchenko, J. W. Hovenier, and L. D. Travis, eds. (Academic, San Diego, Calif., 1999), pp. 481–524.
5. P. W. Barber and S. C. Hill, *Light Scattering by Particles: Computational Methods* (World Scientific, Singapore, 1990).
6. W. J. Wiscombe and A. Mugnai, "Single scattering from nonspherical Chebyshev particles: a compendium of calculations," *NASA Ref. Publ.* **1157** (1986).
7. D. A. Varshalovich, A. N. Moskalev, and V. K. Khersonskii, *Quantum Theory of Angular Momentum* (World Scientific, Singapore, 1988).
8. P. C. Waterman, "Symmetry, unitarity, and geometry in electromagnetic scattering," *Phys. Rev. D* **3**, 825–839 (1971).
9. M. I. Mishchenko, L. D. Travis, and D. W. Mackowski, "T-matrix computations of light scattering by nonspherical particles: a review," *J. Quant. Spectrosc. Radiat. Transfer* **55**, 535–575 (1996).
10. J. V. Dave and B. H. Armstrong, "Computation of high-order associated Legendre polynomials," *J. Quant. Spectrosc. Radiat. Transfer* **10**, 557–562 (1970).
11. M. I. Mishchenko and L. D. Travis, "Capabilities and limitations of a current FORTRAN implementation of the T-matrix method for randomly oriented rotationally symmetric scatterers," *J. Quant. Spectrosc. Radiat. Transfer* **60**, 309–324 (1998).
12. C. C. Chuang and K. V. Beard, "A numerical model for the equilibrium shape of electrified raindrops," *J. Atmos. Sci.* **47**, 1374–1389 (1990).
13. K. Aydin, "Centimeter and millimeter wave scattering from nonspherical hydrometeors," in *Light Scattering by Nonspherical Particles: Theory, Measurements, and Applications*, M. I. Mishchenko, J. W. Hovenier, and L. D. Travis, eds. (Academic, San Diego, Calif., 1999), pp. 451–479.
14. M. I. Mishchenko, "Light scattering by randomly oriented rotationally symmetric particles," *J. Opt. Soc. Am. A* **8**, 871–882 (1991).